CMS Physics Analysis Summary

Contact: cms-pag-conveners-smp@cern.ch 2015/12/15

Measurement of the differential cross section of Z boson production in association with jets in proton-proton collisions at $\sqrt{s} = 13$ TeV

The CMS Collaboration

Abstract

Differential cross section measurements of the $Z(\rightarrow \mu\mu)$ boson production in association with jets are presented, using 13 TeV proton-proton collisions data recorded by the CMS detector at the LHC, corresponding to an integrated luminosity of 2.5 fb^{-1}. The cross sections are presented as a function of jet multiplicity, the jet transverse momenta, and the jet rapidity for different jet multiplicities. The cross section measurements are then compared with the predictions from a multileg next-to-leading-order Monte Carlo generator.

1 Introduction

The production of a Z boson in association with hadronic jets is a cardinal process at the LHC providing a reference both for the physics measurements and for the understanding of the detector response. With the large energy in the center-of-mass of the colliding hadrons obtained with the LHC, jet production is present in almost all the processes under study. The decay of the Z boson to charged leptons (here two muons) allows for a clean and efficient selection of a signal sample, contaminated with only a marginal amount of background, and offering therefore the ideal conditions for the study of hadronic jet production. The cross section measurement provides stringent tests of perturbative QCD (pQCD) and of corresponding Monte Carlo (MC) simulations. The production of $Z+$ jets is also an important background to a number of Standard Model (SM) processes (single top, $t\bar{t}$, vector boson fusion, WW scattering, and Higgs boson production) as well as a prominent background in many searches for physics beyond the SM, such as supersymmetry. Therefore it is crucial that the $Z+$ jets cross section be measured as a function of various relevant kinematic variables with the highest possible precision with 13 TeV data.

The cross section of this process has been previously measured at lower energies, by CDF and D0 collaborations with proton-antiproton ($p\bar{p}$) collisions at a centre-of-mass energy $\sqrt{s} =$ 1.96 TeV [1, 2] and by ATLAS and CMS collaborations from proton-proton (pp) collisions at centre-of-mass energy $\sqrt{s} = 7$ TeV [3–6].

2 Data and simulated samples

This analysis is based on $\sqrt{s}$ =13 TeV proton-proton collisions data collected by the CMS detector [7] during 2015 with 25 ns minimum proton bunch spacing mode. Events in data are retained if they pass a trigger selection requiring two isolated muons, one with $p_T > 17$ GeV and the second with $p_T > 8$ GeV. This data sample corresponds to an integrated luminosity of $2.5 \pm 0.1\,\text{fb}^{-1}$.

The $Z+$ jets signal process is generated with MADGRAPH5_AMC@NLO (MG5_AMC@NLO), using the FxFx merging scheme [8, 9]. Parton shower and hadronisation are performed with PYTHIA8 [10] using the CUETP8M1 tune [11]. The matrix element (ME) includes $Z + 0, 1, 2$ jets at next-to-leading order (NLO), giving a LO accuracy for $Z + 3$ jets. The NNPDF 3.0 [12] NLO PDF set is used. The total cross section is normalised to the NNLO prediction, $6025.2^{+264.6}_{-247.5}$ pb, calculated with FEWZ [13]. The quoted uncertainties include the theoretical uncertainties, estimated by varying the factorisation and normalisation scales by factors 0.5 and 2, the PDF and α_s uncertainties, estimated using the PDF4LHC recommendation [14, 15] with 4 different NNLO PDF sets, CT10nnlo [16], NNPDF23 [12], HERAPDF15NNLO [17], MSTW2008nnlo68cl [18].

The $t\bar{t}$ and single top backgrounds are generated using POWHEG [19–21] interfaced to PYTHIA8. Background MC samples corresponding to double vector boson electroweak production (denoted VV in the figure legends) are generated either with MG5_AMC@NLO (WZ) or POWHEG (WW), both interfaced to PYTHIA8, or with PYTHIA8 alone (ZZ). The background from W boson production in association with jets (denoted W in the figure legends) is simulated with MG5_AMC@NLO using the FxFx merging scheme with the same parton multiplicity and order in the ME than for the signal sample.

3 Event Selection

The final state particles in Z + jets decays are identified and reconstructed with the particle-flow (PF) event algorithm [22, 23], which optimally combines the information from the various elements of the CMS detector.

Events whose two highest-p_{T} isolated muons have opposite charges and form a dimuon system with an invariant mass in the 91 ± 20 GeV window are retained. Muon are reconstructed and identified using the *Global Muon* reconstruction and *Tight Muon selection* described in reference [24]. To further suppress cosmic muons, muons from decays in flight, and muons from pileup events, we also require the longitudinal impact parameter with respect to the primary vertex to be less than 5 mm. Muons are retained for the measurement if they have $p_{\mathrm{T}} > 20$ GeV and $|\eta| < 2.4$. To suppress muons that do not originate from the decay of the Z boson, an isolation requirement is imposed:

$$R_{iso} = [\sum^{charged} p_{\mathrm{T}} + max(0, \sum^{neutral} p_{\mathrm{T}} + \sum^{\gamma} p_{\mathrm{T}} - 0.5 \sum^{PU} p_{\mathrm{T}})] / p_{\mathrm{T}}^{\mu} \leq 0.25, \quad (1)$$

where the sums run over PF candidates in a cone of radius $\Delta R = \sqrt{(\Delta\phi)^2 + (\Delta\eta)^2} = 0.4$ around the direction of the muon candidate track (excluding this track), divided by the muon candidate p_{T}: charged hadrons originating from the primary vertex of the event, neutral hadrons, photons (γ), and charged hadrons not originating from the primary vertex due to pileup events (PU). Since neutral pileup particles deposit collectively on average half as much energy as charged pileup particles, the contamination in the isolation cone from neutral particles coming from pileup interactions is estimated as $0.5 \sum^{PU} p_T$, and it is subtracted in R_{iso}.

Jets are reconstructed by clustering the PF candidates with the anti-k_T algorithm [25, 26] , with a distance parameter of 0.4, and excluding charged particles associated with pileup vertices. Jets are required to have $p_{\mathrm{T}} > 30$ GeV, $|y|$ <2.4, and to have a spatial separation from muon candidates of $\Delta R > 0.4$. Reconstructed jets are corrected with p_{T}, η dependent corrections, calculated on Monte Carlo simulation. An additional residual calibration is applied to the data (η- and p_{T}-dependent) to correct for the differences observed between data and MC.

Jets reconstructed from the pileup despite the vertex requirement used in the jet clustering, are rejected using the output of a multivariate analysis of discriminant variables described in reference [27]. For a more realistic simulation of the pileup conditions present in our data sample, the simulated events are reweighted using the observed distribution of the number of pileup interactions for an optimal pileup modelling.

4 Backgrounds estimate

All background processes are simulated by MC event generators, normalised to their highest order calculated SM cross section, as described in Section 2. The Z decay in $\tau^+\tau^-$ is considered as background and is subtracted during the unfolding procedure described in Sec. 6. The background contamination is below the percent level for the inclusive selection, but increases with the number of jets mainly due to $\mathrm{t\bar{t}}$ production, reaching 15% for a jet multiplicity of 4 and above, as shown in Fig. 3.

The estimated background yields are subtracted from data before unfolding.

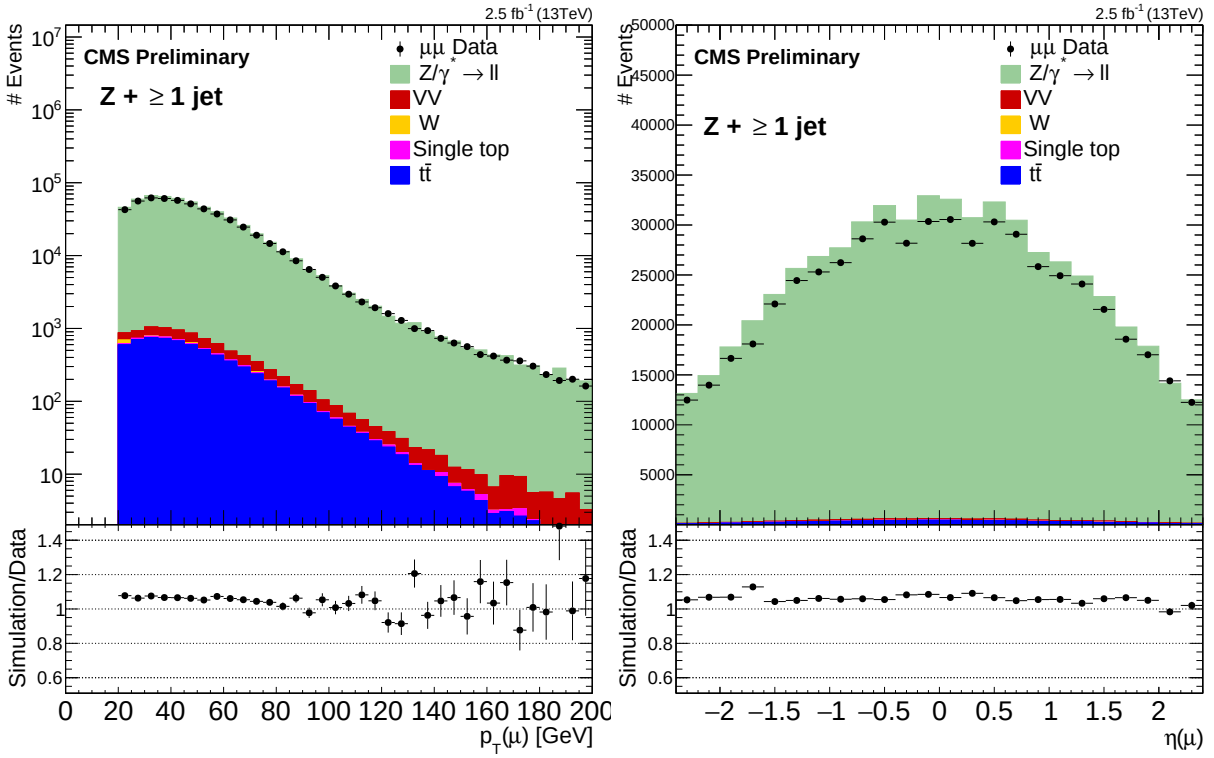

Figure 1: Reconstructed data and simulated signal and backgrounds distributions of muon transverse momenta, $p_{\mathrm{T}}(\mu)$, and pseudo-rapidity, $\eta(\mu)$ for Z + $\geq$ 1 jet events passing the measurement selection. The error bars on the data points correspond to the statistical errors (in the case of the ratio plots, they correspond to the statistical errors coming from both the data and the simulation).

5 Comparison of data and simulation

The agreement between simulation and data is shown in this section for the variables used in the event selection, and for the variables we use in the measurement of the differential cross section. The data are compared to the sum of the simulation contributions from signal and backgrounds. Each figure also shows the ratio of simulation to data. Only statistical uncertainties on the data points are shown.

The distributions of the muon transverse momenta (p_{T}), and pseudo-rapidity are shown in Fig. 1 for the inclusive one jet multiplicities. Reasonable agreement between data and simulation is found over the full phase space. Because of the jet requirement, the overall normalisation depends on the jet energy scale, whose uncertainty, as other systematic uncertainties, is not included in the plots. The difference observed here is actually not present when no jet requirement is applied.

The energy-momentum four vector of the Z boson candidate is reconstructed as the sum of the four vectors of the muon candidates with the two highest transverse momenta and opposite charges. The invariant mass and rapidity of the reconstructed Z boson candidates are shown in Fig. 2 for the inclusive one jet multiplicity.

The comparison of jet multiplicities is presented in Fig. 3 for inclusive multiplicity (left) and exclusive multiplicity (right). The number of events in each bin of the exclusive jet multiplicity for both data and MC signal and backgrounds are listed in Tab. 1.

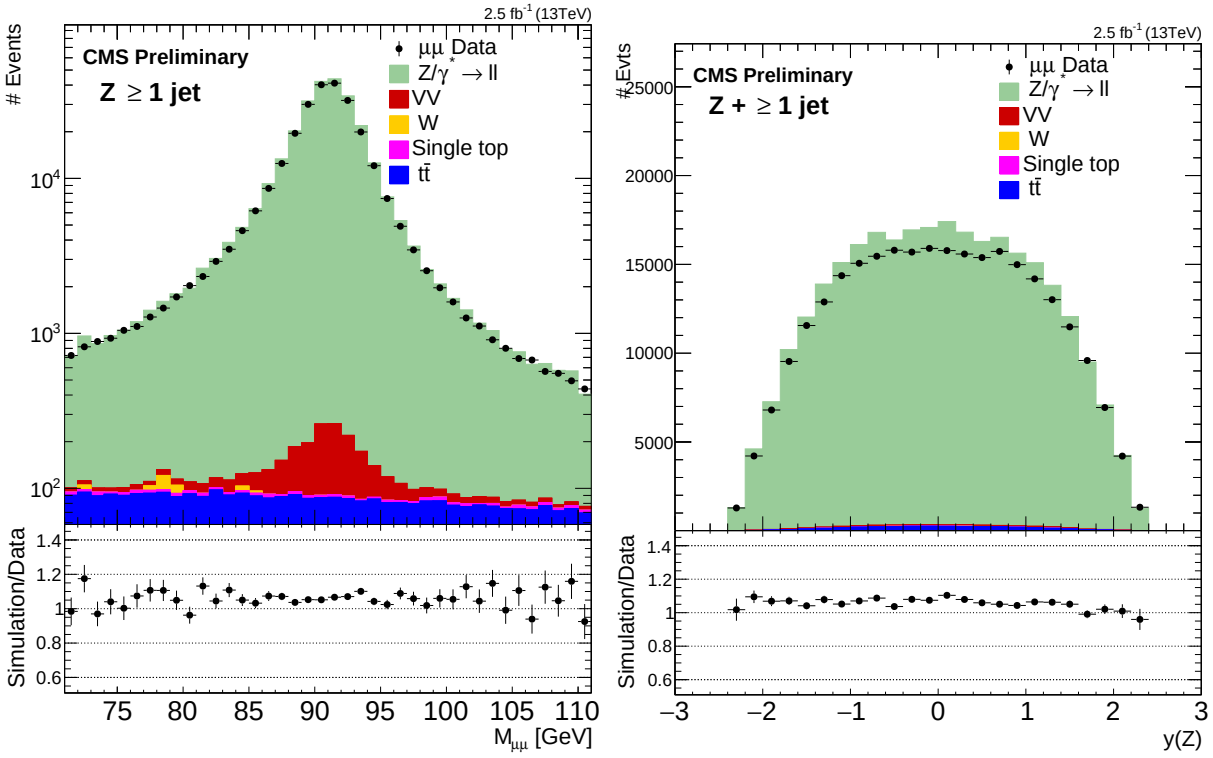

Figure 2: Reconstructed data and simulated signal and backgrounds distributions of the Z candidate invariant mass and rapidity for Z + $\geq$ 1 jet events passing the measurement selection. The error bars on the data points correspond to the statistical errors (in the case of the ratio plots, they correspond to the statistical errors coming from both the data and the simulation).

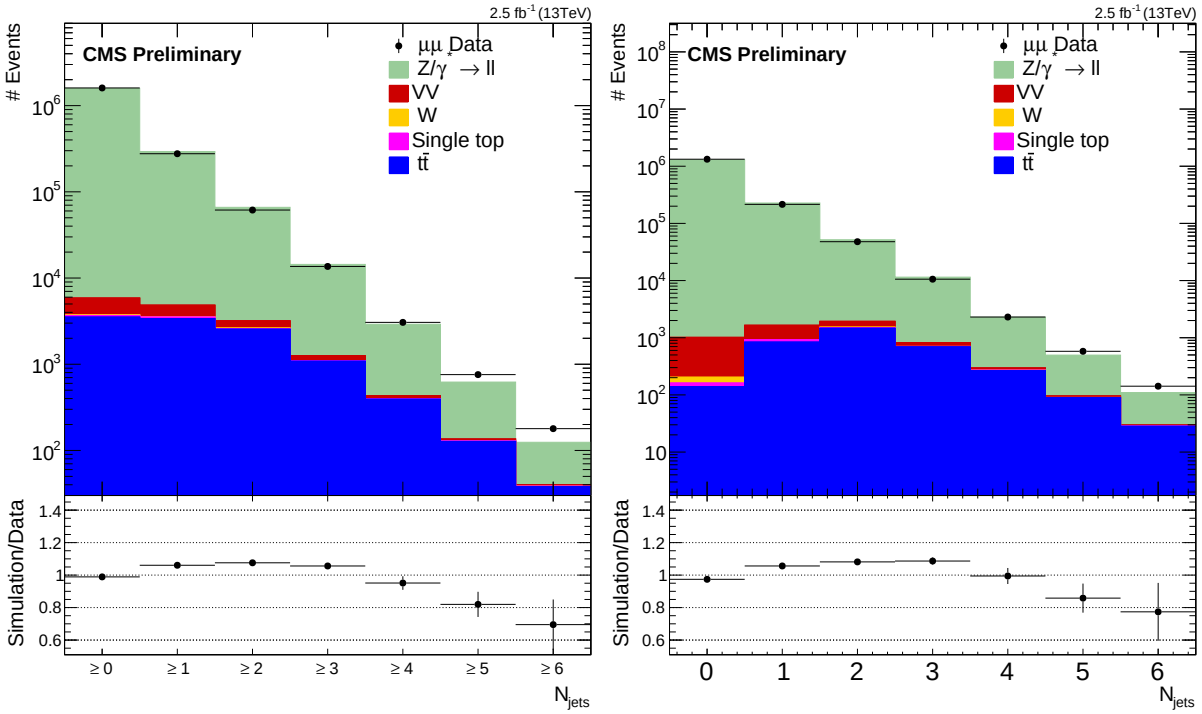

Figure 3: Reconstructed data and simulated signal and backgrounds distributions of (left) the inclusive jet multiplicity and (right) exclusive jet multiplicity. The error bars on the data points correspond to the statistical errors (in the case of the ratio plots, they correspond to the statistical errors coming from both the data and the simulation).

Table 1: Number of events in data and MC samples for the exclusive jet multiplicity after the full selection

	$N_{\text{jets}} = 0$	$N_{\text{jets}} = 1$	$N_{\text{jets}} = 2$	$N_{\text{jets}} = 3$	$N_{\text{jets}} = 4$	$N_{\text{jets}} = 5$	$N_{\text{jets}} = 6$	$N_{\text{jets}} = 7$
TT	140	845	1477	697	267	90	28	7
Single Top	40	151	63	24	11	1	0	0
ZZ	301	320	201	62	13	3	1	0
WW	291	91	24	4	1	0	0	0
WJets	42	0	33	0	0	0	0	0
WZ	238	277	145	42	11	2	0	1
DYJets	1299651	227884	50218	10736	2005	403	79	2
TOTAL	1300703	229568	52161	11565	2308	499	108	10
Data	1326364	215254	47842	10570	2302	579	142	30
Ratio	0.981	1.07	1.09	1.09	1.00	0.86	0.76	0.3

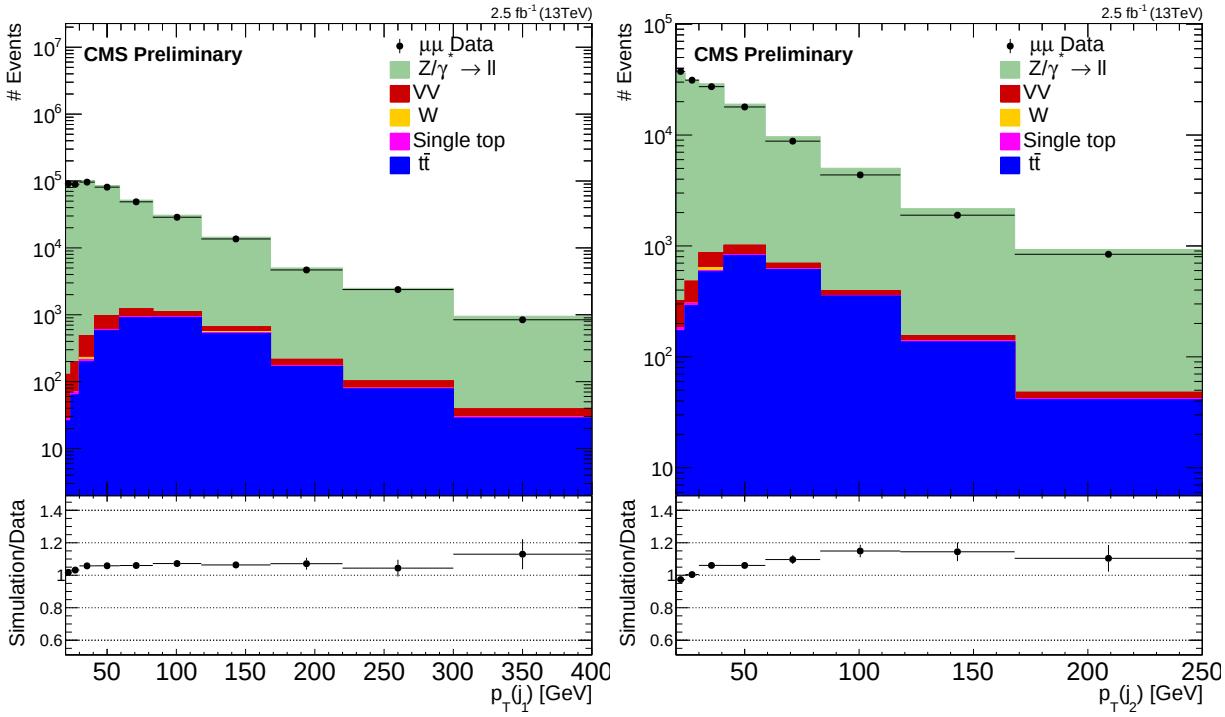

Figure 4: Reconstructed data and simulated signal and backgrounds distributions of the transverse momenta of the two highest p_{T} jets. The error bars on the data points correspond to the statistical errors (in the case of the ratio plots, they correspond to the statistical errors coming from both the data and the simulation).

Due to the limited statistics, the differential jet cross sections are shown only up to the third jet. Fig. 4 and 5 show the data to simulation comparison of the jet transverse momentum for the three highest p_{T} jets. Same comparison can be found for the rapidity of the jets in Fig. 6 and 7. The H_T distributions, representing the scalar sum of the transverse momenta of the considered jets, for inclusive jet multiplicities from one to three are shown in Fig. 8 and 9.

6 Unfolding procedure

The fiducial cross sections are obtained by subtracting the simulated backgrounds from the data distributions, and correcting the background-subtracted data distributions back to the particle level using an unfolding procedure. This procedure takes into account detector effects

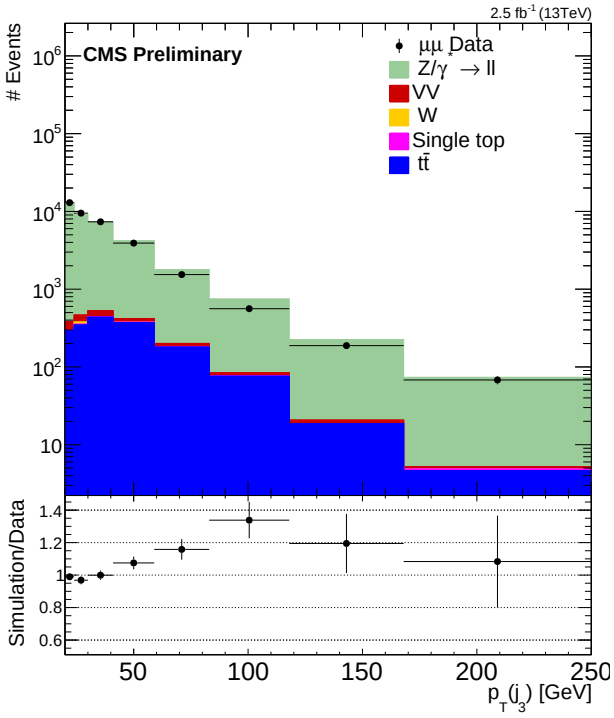

Figure 5: Reconstructed data and simulated signal and backgrounds distributions of the transverse momenta of the third highest p_{T} jet. The error bars on the data points correspond to the statistical errors (in the case of the ratio plots, they correspond to the statistical errors coming from both the data and the simulation).

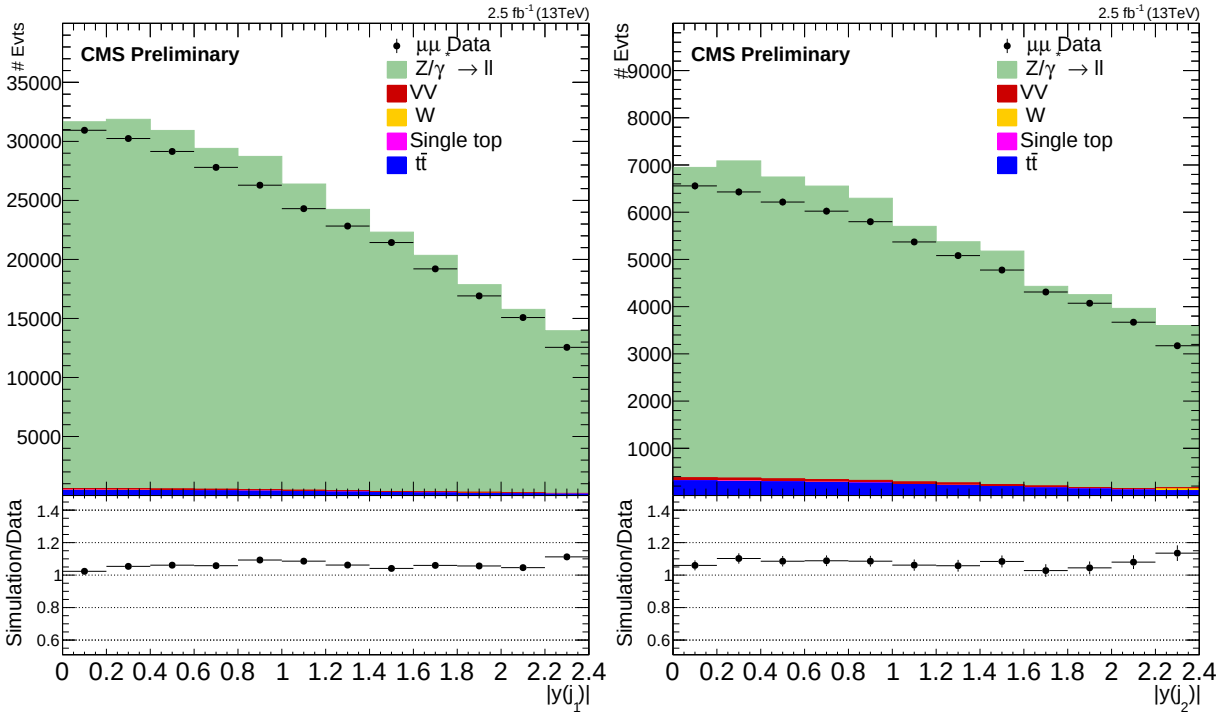

Figure 6: Reconstructed data and simulated signal and backgrounds distributions of the rapidity of the two highest p_{T} jets. The error bars on the data points correspond to the statistical errors (in the case of the ratio plots, they correspond to the statistical errors coming from both the data and the simulation).

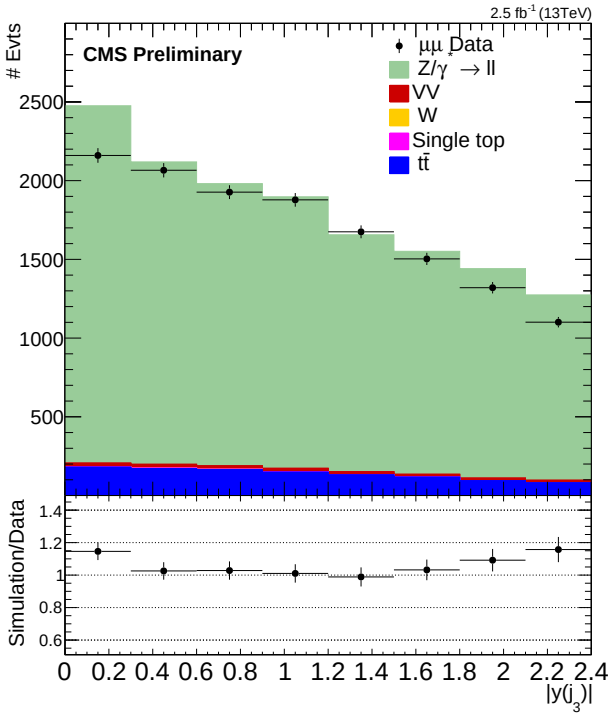

Figure 7: Reconstructed data and simulated signal and backgrounds distributions of the rapidity of the third highest p_{T} jet. The error bars on the data points correspond to the statistical errors (in the case of the ratio plots, they correspond to the statistical errors coming from both the data and the simulation).

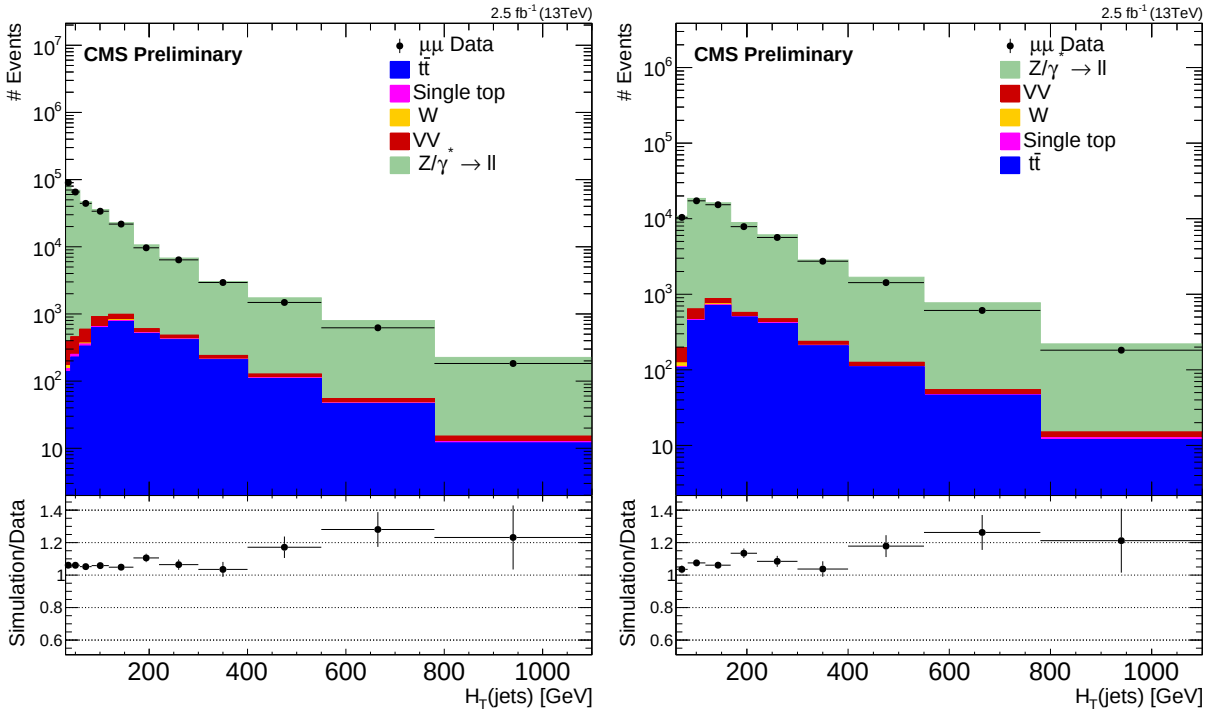

Figure 8: Data to simulation comparison of H_T of the jets for inclusive jet multiplicities of one and two. The error bars on the data points correspond to the statistical errors (in the case of the ratio plots, they correspond to the statistical errors coming from both the data and the simulation).

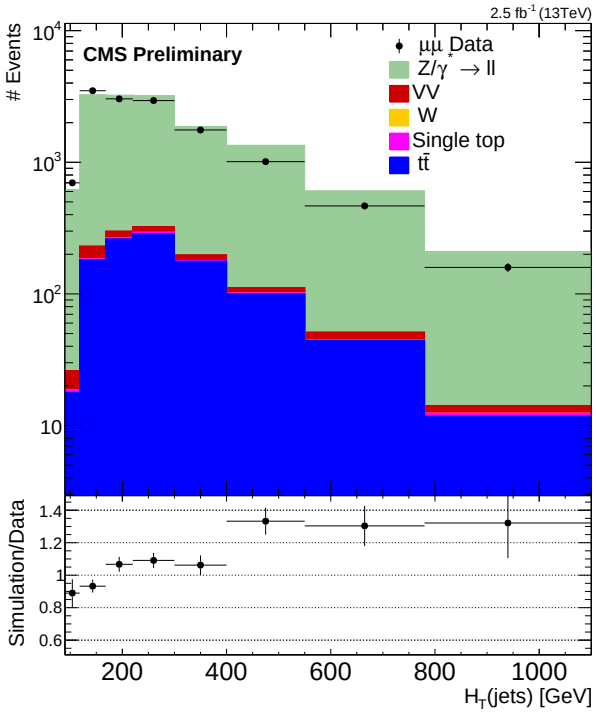

Figure 9: Data to simulation comparison of H_T of the jets for inclusive jet multiplicities of three. The error bars on the data points correspond to the statistical errors (in the case of the ratio plots, they correspond to the statistical errors coming from both the data and the simulation).

such as detection efficiency and resolution. The unfolding procedure is performed using the iterative Bayesian method [28] implemented in the RooUnfold toolkit [29]. A response matrix, which defines the migration probability between the particle-level and reconstructed quantities, as well as the overall reconstruction efficiency, is computed using the simulated Z + jets events. The contribution from $Z \to \tau^+\tau^-$ events and from $Z \to \mu^+\mu^-$ events outside of the measurement phase space but passing the event selection is subtracted together with the background before performing the unfolding.

The particle-level objects refer to the stable muons from the decay of Z boson and to the generator-level hadrons on which the anti-k_T algorithm (size parameter of 0.4) has been applied to obtain the generated jets. The momenta of all the photons whose ΔR distance to the muons axis is smaller than 0.1 are added to the muon momentum to account for the effects of the final state radiation. The lepton is said to be "dressed". Using the dressed muon kinematics, the Z boson is reconstructed. The phase space for the cross section measurement is restricted to events with $p_T > 20\,\text{GeV}$ and $|\eta| < 2.4$ for both muons, and with a dimuon mass within 71 GeV and 111 GeV.

7 Systematic uncertainties

The dominant source of systematic uncertainty is the jet energy scale uncertainty, which is estimated by assigning a p_T- and η-dependent uncertainty, and by varying the jet p_T in data by the magnitude of the uncertainty. These uncertainties amount to 7 % for a jet multiplicity of 1, and increase with the number of reconstructed jets.

The uncertainty on the cross section of the largest background contribution from top pairs,

is estimated to be 10%. The resulting uncertainty from the cross section variation on the jet multiplicity measurement ranges from 0.09% to 1.5% for jet multiplicities 1 through 4.

A systematic uncertainty associated with the generator used to build the unfolding response matrix is assessed by weighting the simulation to agree with the data in each distribution and constructing a reweighted response matrix to unfold the data. The reweighting is done using a finer binning allowing to be sensitive to different shapes within bins. The difference between the unfolded results obtained using the weighted response matrix and the nominal results is taken as the systematic uncertainty associated with the unfolding response matrix.

The jet energy resolution uncertainty has been estimated for data and simulation. The resulting uncertainty on the measurement is of the order of 1%. The uncertainty of the pile-up model results in an uncertainty on the measurement of the same order.

Finally, the uncertainty on the integrated luminosity is 4.6%.

8 Results

The measured $Z+$ jets cross sections are shown in Fig. 10 to 16 in comparison with the prediction of MG5_AMC@NLO. Fig. 10 shows the measured cross section as a function of the jets inclusive and exclusive multiplicity. Good agreement between reconstructed data and simulation is observed up to four jets. Good agreement is to be expected up to three jets since the MG5_AMC@NLO sample was generated for two partons in the final state at NLO. Above a multiplicity of three, the jets are simulated only by the parton shower of PYTHIA8.

Figures 11 and 12 show the measured cross section as a function of the transverse momentum of the three leading p_{T} jets, Fig. 15 and 16 show it as a function of their rapidity, and Fig. 13 and 14 show it as a function of H_T for inclusive jet multiplicities from one to three. All data distributions are well reproduced by the simulation, although the third jet p_{T} is decreasing a little more rapidly in data than simulation.

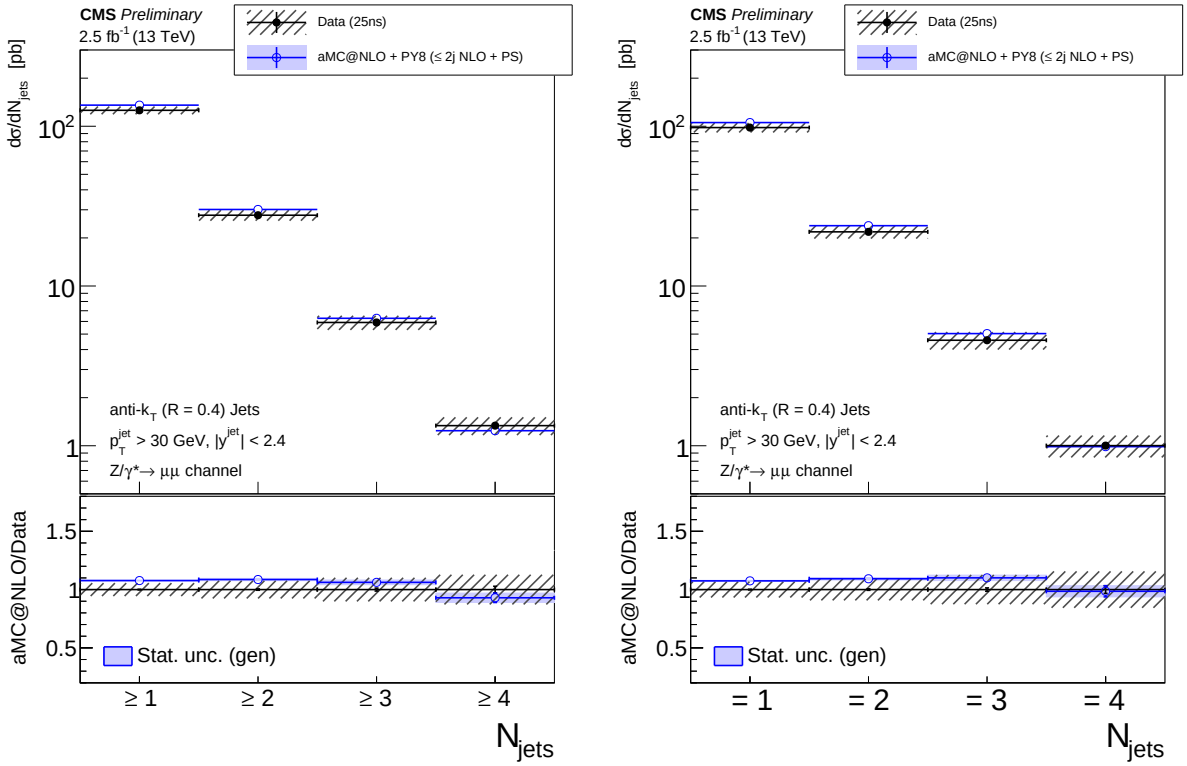

Figure 10: Measured cross section as a function of (left) the jets inclusive and (right) exclusive multiplicity. The error bar represents the statistical uncertainty and the grey hatched band represents the total uncertainty including systematic and statistical uncertainties.

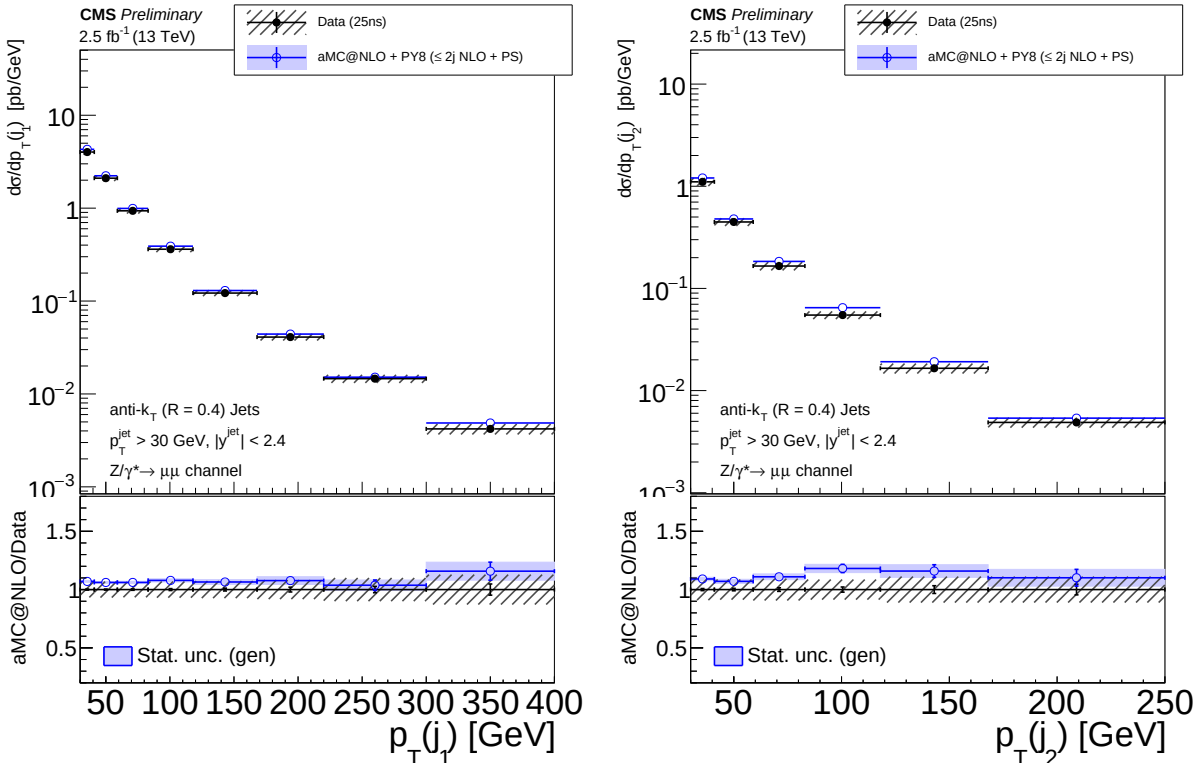

Figure 11: Measured cross section as a function of the p_{T} of (left) the first and (right) the second jets. The error bar represents the statistical uncertainty and the grey hatched band represents the total uncertainty including systematic and statistical uncertainties.

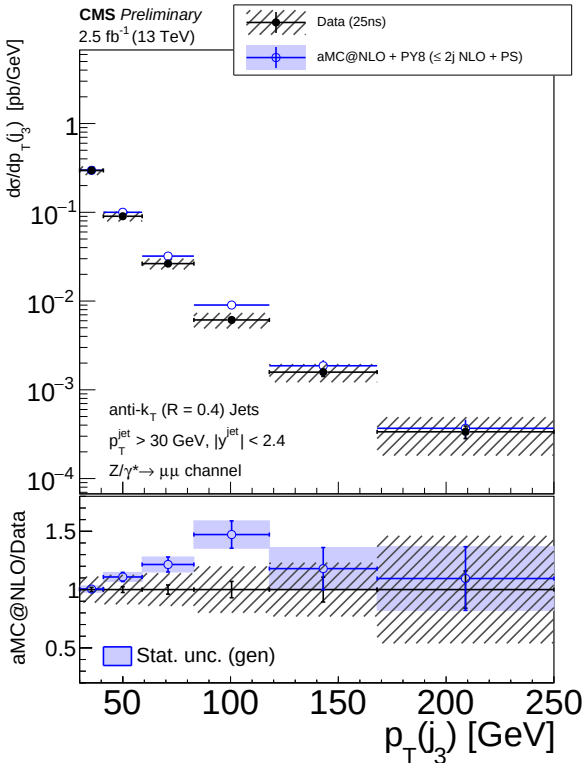

Figure 12: Measured cross section as a function of the p_{T} of the third jet. The error bar represents the statistical uncertainty and the grey hatched band represents the total uncertainty including systematic and statistical uncertainties.

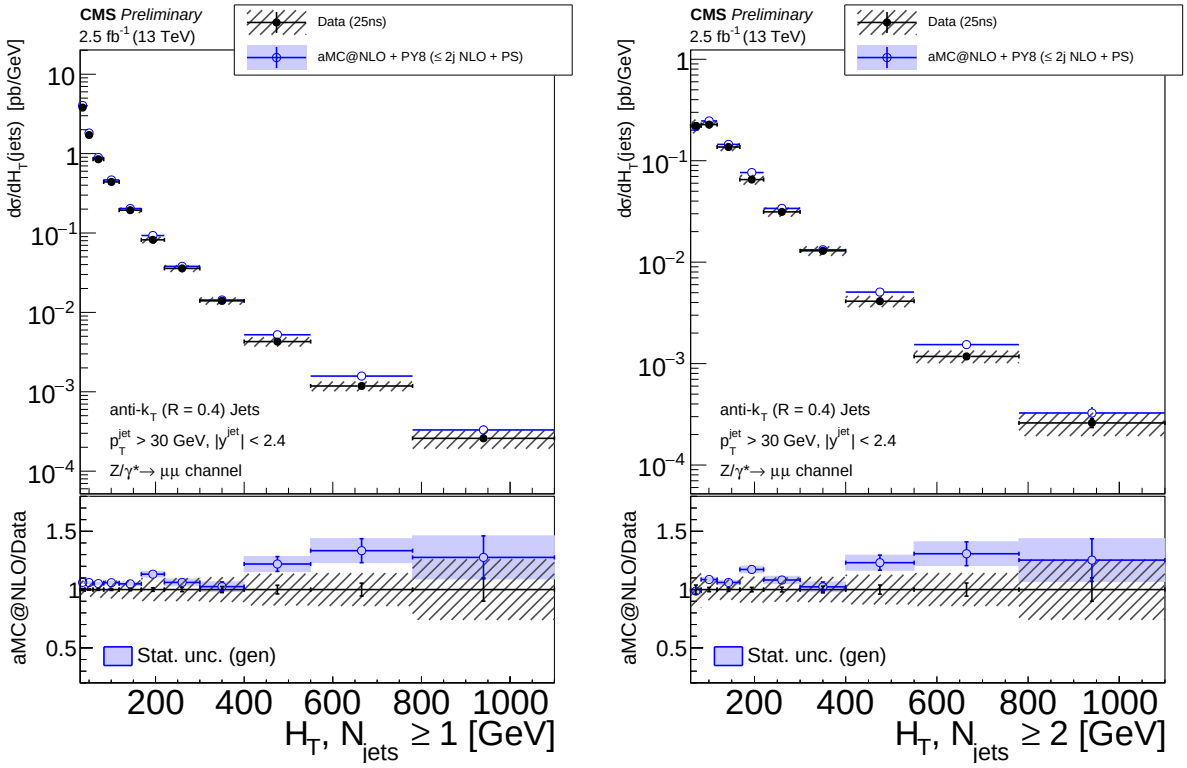

Figure 13: Measured cross section as a function of H_T for inclusive jet multiplicities of (left) one and (right) two. The error bar represents the statistical uncertainty and the grey hatched band represents the total uncertainty including systematic and statistical uncertainties.

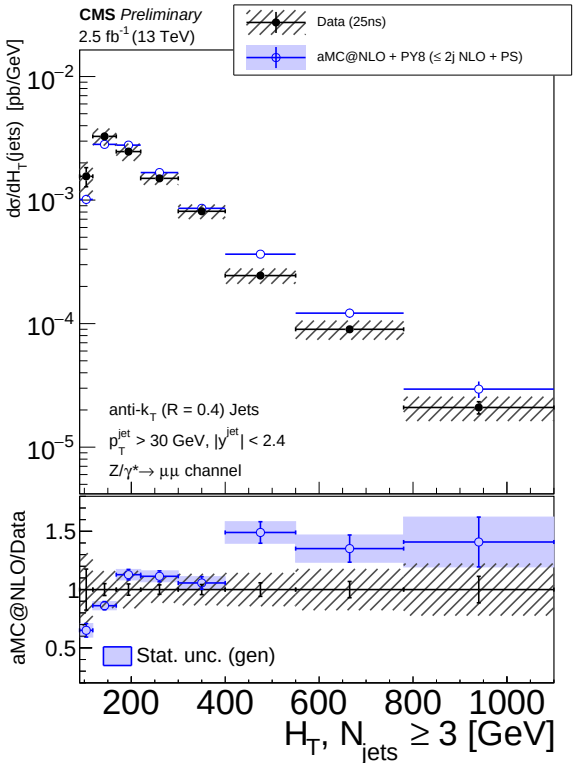

Figure 14: Measured cross section as a function of H_T for inclusive jet multiplicities of three. The error bar represents the statistical uncertainty and the grey hatched band represents the total uncertainty including systematic and statistical uncertainties.

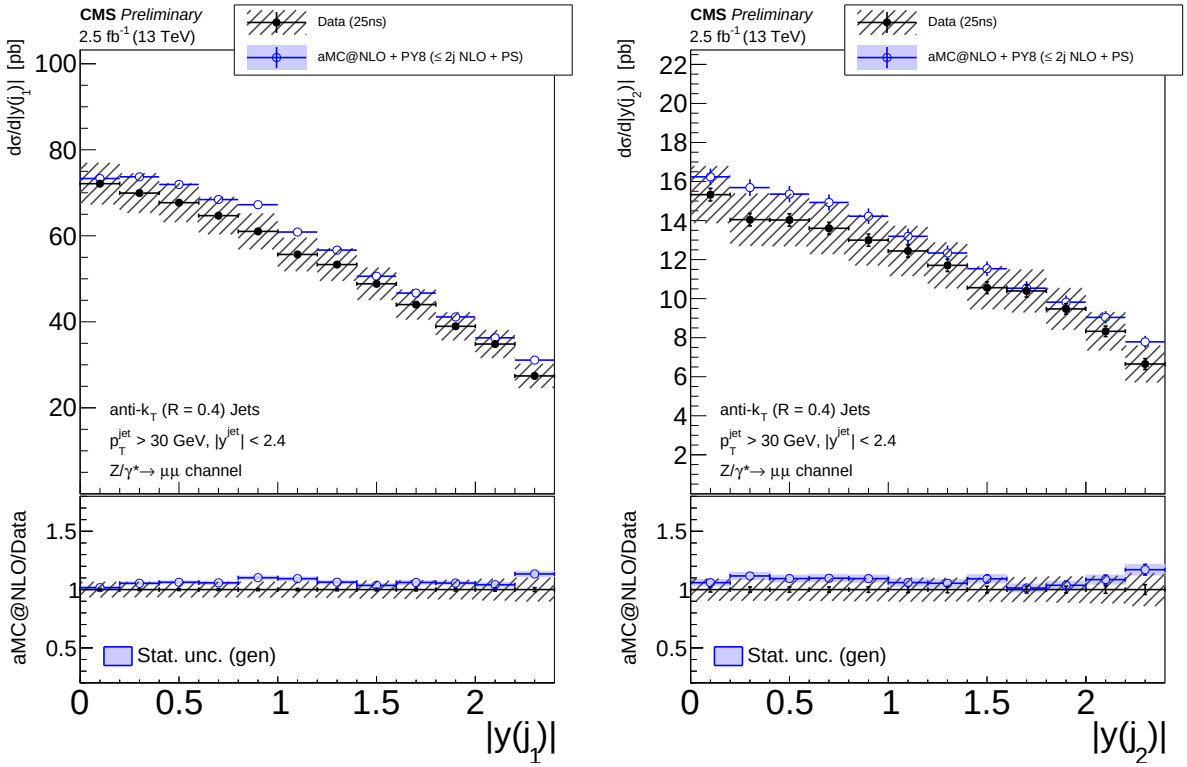

Figure 15: Measured cross section as a function of the rapidity of the (right) first and (left) second highest p_{T} jets. The error bar represents the statistical uncertainty and the grey hatched band represents the total uncertainty including systematic and statistical uncertainties.

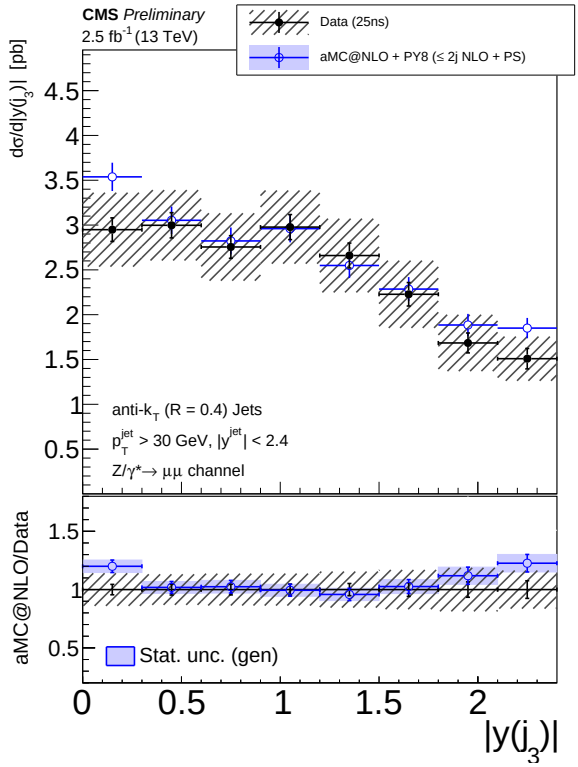

Figure 16: Measured cross section as a function of the rapidity of the third highest p_{T} jet. The error bar represents the statistical uncertainty and the grey hatched band represents the total uncertainty including systematic and statistical uncertainties.

9 Summary

Measurements of the cross sections and differential cross sections for a Z boson produced in association with jets in pp collisions at a centre-of-mass energy of 13 TeV are presented. The data correspond to an integrated luminosity of 2.5 fb^{-1} and were collected with the CMS detector during the 2015 proton-proton run with 25 ns bunch crossing at the LHC.

Cross sections determined using the dimuon decay mode of the Z boson are presented as functions of the jet multiplicity, the p_{T} and rapidities of the three leading jets as well as H_T for inclusive jet multiplicities from one to three.

The results are corrected for all detector effects using regularised unfolding and compared with the predictions of NLO pQCD with parton showering and detector simulation. The predictions generally describe the measured cross sections within the uncertainties.

References

[1] CDF Collaboration, "Measurement of inclusive jet cross sections in $Z/\gamma^* \to e^+e^-$ + jets production in $p\bar{p}$ collisions at $\sqrt{s}$ = 1.96 TeV", *Phys. Rev. Lett.* **100** (Mar, 2008) 102001, doi:10.1103/PhysRevLett.100.102001.

[2] D0 Collaboration, "Measurement of differential Z/γ^* + jet + X cross sections in $p\bar{p}$ collisions at $\sqrt{s}$ = 1.96 TeV", *Phys. Lett.* **B669** (2008) 278–286, doi:10.1016/j.physletb.2008.09.060, arXiv:0808.1296.

[3] ATLAS Collaboration, "Measurement of the production cross section of jets in association with a Z boson in pp collisions at $\sqrt{s} = 7$ TeV with the ATLAS detector", *JHEP* **1307** (2013) 032, doi:10.1007/JHEP07(2013)032, arXiv:1304.7098.

[4] ATLAS Collaboration, "Measurement of the production cross section for Z/γ^* in association with jets in pp collisions at $\sqrt{s} = 7$ TeV with the ATLAS detector", *Phys. Rev. D* **85** (2012) 032009, doi:10.1103/PhysRevD.85.032009.

[5] CMS Collaboration, "Jet Production Rates in Association with W and Z Bosons in pp Collisions at $\sqrt{s} = 7$ TeV", *JHEP* **1201** (2012) 010, doi:10.1007/JHEP01(2012)010, arXiv:1110.3226.

[6] CMS Collaboration, "Measurements of jet multiplicity and differential production cross sections of Z+ jets events in proton-proton collisions at $\sqrt{s} = 7$ TeV", *Phys.Rev.* **D91** (2015), no. 5, 052008, doi:10.1103/PhysRevD.91.052008, arXiv:1408.3104.

[7] CMS Collaboration, "The CMS experiment at the CERN LHC", *JINST* **3** (2008) S08004, doi:10.1088/1748-0221/3/08/S08004.

[8] J. Alwall et al., "The automated computation of tree-level and next-to-leading order differential cross sections, and their matching to parton shower simulations", *JHEP* **07** (2014) 079, doi:10.1007/JHEP07(2014)079, arXiv:1405.0301.

[9] S. F. Rikkert Frederix, "Merging meets matching in MC@NLO", doi:10.1007/JHEP12(2012)061, arXiv:1209.6215.

[10] T. Sjostrand, S. Mrenna, and P. Z. Skands, "A Brief Introduction to PYTHIA 8.1", *Comput. Phys. Commun.* **178** (2008) 852–867, doi:10.1016/j.cpc.2008.01.036, arXiv:0710.3820.

[11] CMS Collaboration, "Event generator tunes obtained from underlying event and multiparton scattering measurements", arXiv:1512.00815.

[12] NNPDF Collaboration, "Parton distributions for the LHC Run II", *JHEP* **04** (2015) 040, doi:10.1007/JHEP04(2015)040, arXiv:1410.8849.

[13] K. Melnikov and F. Petriello, "Electroweak gauge boson production at hadron colliders through O(alpha(s)**2)", *Phys. Rev.* **D74** (2006) 114017, doi:10.1103/PhysRevD.74.114017, arXiv:hep-ph/0609070.

[14] M. Botje et al., "The PDF4LHC Working Group Interim Recommendations", arXiv:1101.0538.

[15] S. Alekhin et al., "The PDF4LHC Working Group Interim Report", arXiv:1101.0536.

[16] R. D. Ball et al., "CT10 next-to-next-to-leading order global analysis of QCD", *Phys. Rev.D* **89** (2014) 033009, arXiv:arXiv:1302.6246.

[17] H1 and ZEUS Collaboration Collaboration, "PDF Fits at HERA", *PoS EPS-HEP2011* (2011) 320, arXiv:arXiv:1112.2107.

[18] A. D. Martin, S. W. J., T. R. S., and G. Watt, "Parton distributions for the LHC", *Eur. Phys. J. C* **63** (2009) 189, arXiv:arXiv:0901.0002.

[19] P. Nason, "A New method for combining NLO QCD with shower Monte Carlo algorithms", *JHEP* **11** (2004) 040, doi:10.1088/1126-6708/2004/11/040, arXiv:hep-ph/0409146.

[20] S. Frixione, P. Nason, and C. Oleari, "Matching NLO QCD computations with Parton Shower simulations: the POWHEG method", *JHEP* **11** (2007) 070, doi:10.1088/1126-6708/2007/11/070, arXiv:0709.2092.

[21] S. Alioli, P. Nason, C. Oleari, and E. Re, "A general framework for implementing NLO calculations in shower Monte Carlo programs: the POWHEG BOX", *JHEP* **06** (2010) 043, doi:10.1007/JHEP06(2010)043, arXiv:1002.2581.

[22] CMS Collaboration, "Particle-flow event reconstruction in CMS and performance for jets, taus, and $E_{\mathrm{T}}^{\mathrm{miss}}$", CMS Physics Analysis Summary CMS-PAS-PFT-09-001, 2009.

[23] CMS Collaboration, "Commissioning of the particle-flow event with the first LHC collisions recorded in the CMS detector", CMS Physics Analysis Summary CMS-PAS-PFT-10-001, 2010.

[24] CMS Collaboration, A. Calderon, "Performance of muon identification and reconstruction with the CMS detector", in *Proceedings, 14th ICATPP Conference on Astroparticle, Particle, Space Physics and Detectors for Physics Applications (ICATPP 2013)*, pp. 332–336. 2014. doi:10.1142/9789814603164_0050.

[25] M. Cacciari, G. P. Salam, and G. Soyez, "The anti-k_t jet clustering algorithm", *JHEP* **04** (2008) 063, doi:10.1088/1126-6708/2008/04/063, arXiv:0802.1189.

[26] M. Cacciari, G. P. Salam, and G. Soyez, "FastJet user manual", *Eur. Phys. J. C* **72** (2012) 1896, doi:10.1140/epjc/s10052-012-1896-2, arXiv:1111.6097.

[27] CMS Collaboration, "Pileup Jet Identification", Technical Report CMS-PAS-JME-13-005, 2013.

[28] G. D'Agostini, "A Multidimensional unfolding method based on Bayes' theorem", *Nucl. Instrum. Meth.* **A362** (1995) 487–498, doi:10.1016/0168-9002(95)00274-X.

[29] T. Adye, "Unfolding algorithms and tests using RooUnfold", in *Proceedings of the PHYSTAT 2011 Workshop, CERN, Geneva, Switzerland, January 2011, CERN-2011-006, pp 313-318*, pp. 313–318. 2011. arXiv:1105.1160.